Auroral Kilometric Radiation: Time-Averaged Source Location

DENNIS L. GALLAGHER AND DONALD A. GURNETT

Department of Physics and Astronomy, University of Iowa, Iowa City, Iowa 52242

The location of the average generation region of auroral kilometric radiation is found by studying average electric field strengths as a function of spacecraft position in narrow frequency bands centered at 178, 100, and 56.2 kHz. A combined 5 years of data from the University of Iowa plasma wave experiments on satellites Hawkeye 1 and Imp 6 provide the basis for determining the average electric field strengths. Hawkeye 1 was in a highly elliptical, polar orbit with an apogee near 21 R_E over the northern polar region, and Imp 6 was in a highly elliptical, near-equatorial orbit with an apogee of 33 R_E. Together these satellites provide extensive coverage from 3 to 21 R_E in the northern hemisphere and inside of 3 R_E in the southern hemisphere. Intense sources of auroral kilometric radiation are found in the northern and southern hemispheres. Their locations are near 65° invariant latitude in their respective hemispheres, between 22 and 24 hours magnetic local time, and near 2.5 R_E. The total time-averaged power generation is found to be about 10^7 W, assuming a spectral bandwidth of 200 kHz. Propagation effects limit the emission cone of auroral kilometric radiation in a given hemisphere to roughly 4.1 sr at 178 kHz, 2.2 sr at 100 kHz, and 1.5 sr at 56.2 kHz. Evidence that the polar cusp region is illuminated at distances as close as 4 R_E suggests the possibility that previously observed polar cusp sources are the result of scattering from field-aligned density irregularities.

1. INTRODUCTION

This study of electric field intensities has been undertaken to resolve uncertainties in the location of intense sources of earth-related kilometric radiation. From the earliest observations by *Benediktov et al.* [1965, 1968], evidence submitted by numerous investigators has pointed to widely varying locations for the origin of the very intense and sporadic kilometric radiation which has a sharply peaked spectrum between 100 and 300 kHz. *Benediktov et al.* [1965, 1968] correlated radio emissions between 0.725 and 2.3 MHz with geomagnetic activity and concluded that the source is near the earth. *Dunckel et al.* [1970] reported that this intense radiation is observed primarily in the local nighttime and is strongly correlated with the auroral electrojet (*AE*) index. A source location in the tail region of the magnetosphere for sporadic noise at 250 kHz was observed by *Stone* [1973]. *Gurnett* [1974] presented a frequency of occurrence study of kilometric radiation showing a conical radiation pattern centered at the earth, at high latitudes in the local evening, and referred to this intense radiation as terrestrial kilometric radiation. Gurnett demonstrated that the observed conical radiation pattern could be explained if the source location of the radiation was on an auroral field line at ≤ 3 R_E (earth radii). Gurnett also showed that the kilometric radiation was closely associated with discrete auroral arcs. The two-component source model proposed by *Kaiser and Stone* [1975] described a less intense, quasi-continuous dayside source in addition to the intense, sporadic nightside source described by Gurnett. Using the direction-finding technique of analyzing spin-modulated electric field intensities from satellites Hawkeye 1 and Imp 8, *Kurth et al.* [1975] reported the average source location of auroral kilometric radiation between 1 and 2 R_E and at about 20 hours magnetic local time. In another experiment, lunar occultations of intense kilometric radiation observed with Rae 2 were used by *Kaiser and Alexander* [1977] to locate apparent source origins. The most intense source observed was the auroral source described by *Kurth et al.* [1975]. Emissions were also observed in the region of the polar cusp and magnetosheath on the dayside of the earth.

Paper number 9A0974.
0148-0227/79/009A-0974$01.00

Such diverse observations of the source locations of the intense kilometric radiation have produced the very difficult task of finding a single mechanism for the generation of the radiation, which will operate under widely varying plasma conditions. Toward resolving the dilemma, *Alexander et al.* [1978] have recently given strong evidence that kilometric radiation generated near the earth at auroral latitudes may be scattered at large distances in the magnetosheath and solar wind, thereby appearing to come from distant sources. Following this explanation of the observation of distant kilometric radiation sources, two types of terrestrial kilometric radiation observations remain to be examined. The strongest component is auroral kilometric radiation, which is known to originate within 5 R_E at auroral latitudes and in the local evening. Other less intense components discussed by *Alexander et al.* [1978] are observed between 5 and 15 R_E and appear to come from sources aligned along a specific family of geomagnetic field lines. An example is the polar cusp sources observed by *Kaiser and Alexander* [1977]. In summary, these studies have found source locations by lunar occultation techniques and by examining spin-modulated electric field intensities. The methods determine the instantaneous positions of apparent sources of intense kilometric radiation. Such an apparent source may represent a generation region of the radiation or scattering from localized inhomogeneities in plasma density.

The present study will determine which regions in the magnetosphere are strong sources of power at kilometric wavelengths. Time-averaged spectral power flux will first be integrated over earth-centered spherical shells. For shells of varying radius the integrals will give the spectral power and geocentric radial distance of regions of power generation. The latitudinal and local time dependences of the averaged spectral power flux will be examined along with a consequence of the $1/R^2$ radial dependence of spectral power flux observed by *Gurnett* [1974] for terrestrial kilometric radiation. As was postulated by *Alexander et al.* [1978], previously observed polar cusp sources may result from field-aligned scattering centers. Since this study utilizes extensive measurements in and near the source region, the resulting source locations are not as sensitive as remote direction-finding measurements to errors aris-

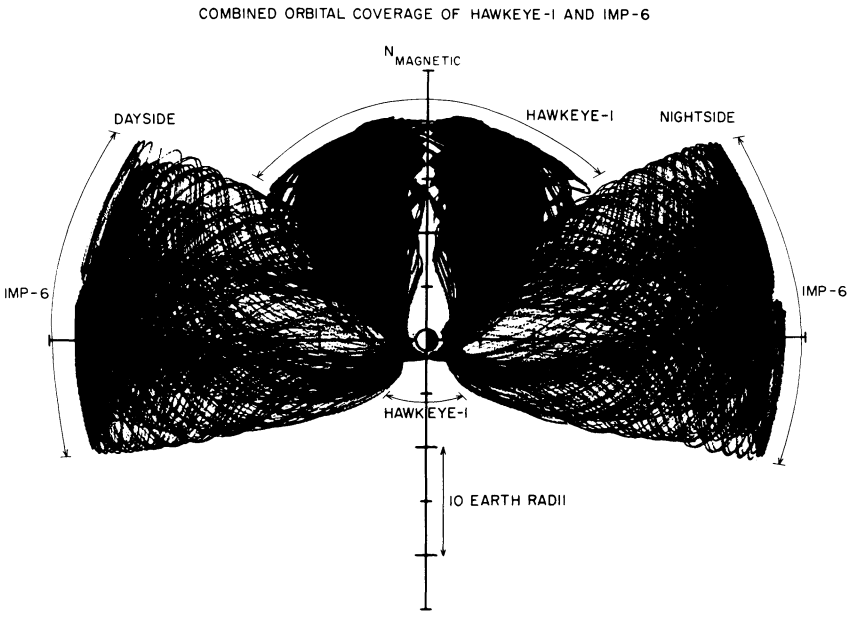

Fig. 1. Combined orbital coverage of Hawkeye 1 and Imp 6. All points on the nightside have been rotated in MLT to form the right side of the figure, and all points on the dayside have been rotated in MLT to form the left side of the figure.

ing from scattering or reflections. The dimensions of observed regions of power generation will also be a measure of the variation in the locations of instantaneous intense sources of kilometric radiation. To the extent that this study better defines those regions which contribute to the energy produced at kilometric wavelengths the generation mechanism for intense kilometric radiation may be sought using a more limited range of plasma parameters than has been possible in the past.

2. Instrumentation

The Hawkeye 1 and Imp 6 satellites have similar plasma wave experiments (described by *Kurth et al.* [1975] and *Gurnett and Shaw* [1973], respectively), which together provide about 5 years of electric field measurements. The combined orbital coverage of the satellites is shown in Figure 1. Locations where measurements are made on the nightside of the earth have been rotated in magnetic local time to form the right side of the figure; all points on the dayside have been rotated to form the left side of the figure. As is shown, northern hemisphere coverage is almost complete out to about 21 R_E. There is no coverage, however, at small radial distances and at high latitudes above the northern pole. Southern hemisphere coverage is limited to latitudes greater than about −40° magnetic latitude except for Hawkeye 1 coverage within 2 R_E.

The success of integrating spectral power flux over spherical shells to find regions of power generation depends strongly upon the completeness of the flux observations over each spherical surface. Such observations cannot satisfactorily be provided by the data from only one satellite. The orbital coverage of satellites Hawkeye 1 and Imp 6 are only partially overlapping. When taken together, the data from these satellites provide an extensive survey of electric field strengths in the vicinity of the earth. Although not shown in Figure 1, the combined orbital coverage extends uniformly throughout all magnetic local times.

3. Data Analysis

Integrating average power flux over earth-centered spherical shells will give an estimate of the geocentric radial distances of the sources of the most intense kilometric radiation and the value of the total average power generation. Using simultaneous observations of electric and magnetic fields by Imp 6, *Gurnett* [1974] showed that electric-to-magnetic field ratios of intense kilometric radiation correspond to that for electromagnetic waves in free space. On this basis an inverse dependence of power flux on the square of radial distance should be observed in the data obtained from satellites Hawkeye 1 and Imp 6. However, the $1/R^2$ dependence of power flux on distance should be seen only as a function of the distance from the origin of the radiation. This origin may be inferred by selecting a source region which yields the power flux dependence of $1/R^2$ that is expected for free space propagating electromagnetic radiation.

Measurements of electric field strength by each satellite are logarithmically compressed and available in the form of a voltage between 0 and 5 V (V_{out}). By using prelaunch calibration tables these measurements are converted to the actual voltages applied to the satellite antennas (V_{in}). From the known effective antenna lengths and filter bandwidths the electric field strength and spectral power flux, P, can be calculated for each measurement. In a study by *Green et al.* [1977] the calibrations on these two satellite instruments were compared through simultaneous observations of type III radio bursts. On the assumption that the satellites were equidistant from the source regions of type III radio bursts the observations of electric field strengths were found to be in close agreement; therefore no normalization is required in averaging measurements of spectral power flux by the two satellites.

For this study the electric field data from Hawkeye 1 and Imp 6 have been averaged over 3-min 4-s and 5-min 28-s intervals, respectively, and as a consequence, spin modulation effects are removed from the data. All data are then averaged into 72 5° increments of magnetic local time (MLT), 36 5° increments of magnetic latitude λ_m, and 15 equal logarithmic increments in geocentric radial distance. This produces a picture of time-averaged spectral power fluxes as a function of position in the vicinity of the earth. The resolution of the picture is limited only by the amount of data available from Hawkeye 1

and Imp 6. For the chosen resolution, there are 10–50 measurements of spectral power flux averaged into each volume element where satellite coverage exists. The objective is for the average of spectral power flux measurements within each volume element to be representative of the average kilometric radiation intensities at each corresponding location. Bursts of kilometric radiation last from tens of minutes to several hours. As a result, some observations within a given volume element will be made when kilometric radiation cannot be observed. By requiring many uncorrelated measurements within a volume element the error in the average intensity is reduced, approximately in proportion to $1/(n)^{1/2}$, where n is the total number of measurements.

As a result of using the electric field data from satellites Hawkeye 1 and Imp 6, over 600,000 measurements of spectral power flux are obtained. Because sources of radiation at kilometric wavelengths such as continuum radiation and type III radio bursts have been observed by *Gurnett* [1974] to be a minor source of energy when compared with terrestrial kilometric radiation, no lower threshold on measurements of spectral power flux will be used to exclude these other forms of kilometric radiation from the present study. An upper threshold can be estimated at respective receiver channel saturations and results in the omission of only four measurements.

Also important is how well measurements of spectral power flux represent the spectral components of the magnitude of the poynting flux. How well an average across the spin-modulated data corresponds to the magnitude of the poynting flux depends ideally on the polarization of the radiation and the orientation of the satellite's axis of rotation. The average of measurements of circularly polarized radiation will yield a result which varies approximately from a factor of 1–0.7 times the magnitude of the electric field component of the radiation. The larger result occurs when the poynting flux direction is along the satellite's axis of rotation. Auroral kilometric radiation is an *R-X* mode propagating radiation as predicted by *Green et al.* [1977] and observed by *Gurnett and Green* [1978] and by *Kaiser et al.* [1978]. Each electric field average will be in error by no more than a factor of about 1.4, and therefore spectral power flux measurements will be in error by no more than a factor of about 2.

The present study could also be influenced by seasonal and long-term variations in kilometric radiation intensities. Seasonal changes are sought by studying separate summer and winter averages of spectral power flux as a function of position. When plots along earth-centered radial vectors of spectral power flux versus distance are made separately for the summer and winter, no statistical differences are found. A possible source of long-term variations is the 11-year solar sunspot cycle. Data are taken from satellites Imp 6 and Hawkeye 1, which provide 7 years of almost nonoverlapping temporal coverage. A solar minimum occurred midway through those 7 years; therefore measurements from these two satellites were made during similar phases of the solar cycle. The effect is expected to mask solar cycle related variations in kilometric radiation intensities if such a variation exists. Consequently, the data examined in this study constitute, as well as possible, an unbiased representation of spectral power flux intensities in the vicinity of the earth.

Assume initially that the picture proposed by *Gurnett* [1974] is generally accurate in describing the locations of the most intense sources of kilometric radiation. The sources of intense kilometric radiation are shown in Gurnett's Figure 14 to be very close to the earth and at high latitudes on auroral field

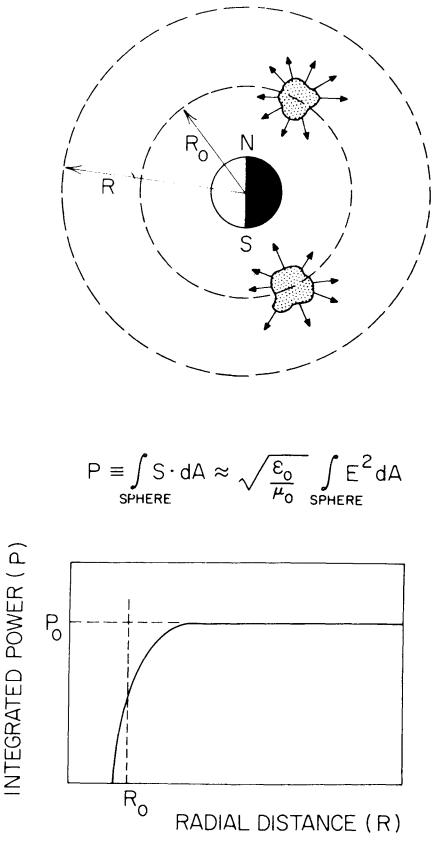

Fig. 2. The integration of poynting flux over concentric, earth-centered, spherical shells for model auroral kilometric radiation sources is shown. Poynting flux magnitudes must be approximated by measurements of spectral power flux. P_0 corresponds to the total power generated by the sources, and R_0 approximately marks the radial distance of the sources from the center of the earth.

lines. If these northern and southern sources of auroral kilometric radiation, as termed by *Kurth et al.* [1975], are well confined, then an integration of the poynting flux over spherical shells which completely enclose the source regions should yield a constant power as shown in Figure 2. If both sources could always be seen, this constant would be equal to the total spectral power generated at the frequency for which the data were chosen. As the radius of these concentric, spherical, earth-centered shells become small, a radius will be reached where they no longer completely enclose the generation regions. As this occurs, the integrated power will fall off at a rate which reflects how well, on the average, the source is confined within the shell of integration. The radii of shells during which this drop off occurs define the location of the source regions in earth-centered radial distance. Poynting flux, however, is not available from both satellites. Instead, measurements of average spectral power flux are used to perform the integrations:

$$\int_{\text{sphere}} \mathbf{S} \cdot d\mathbf{A} \approx \int P\, dA = \left(\frac{\epsilon_0}{\mu_0}\right)^{1/2} \int E^2\, dA\, (\epsilon_0/\mu_0)^{1/2} \approx 1/377$$

where $\mathbf{S}$ is the spectral poynting vector and P is the spectral power flux. The effect of introducing this approximation will be discussed later.

To perform the integration, all volume elements must contain a measurement of spectral power flux. Orbital coverage, however, was not 100% complete, as shown in Figure 1. To compensate, those volume elements for which there are no

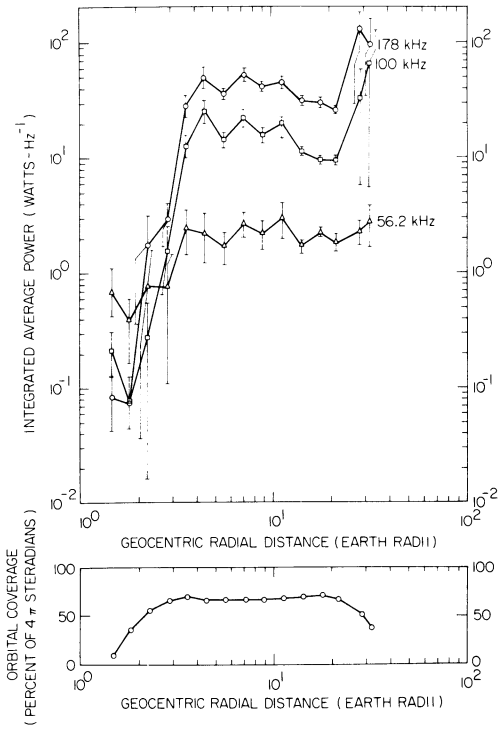

Fig. 3. The integration of observed spectral power flux across concentric, earth-centered, spherical shells is shown in the upper graph. The radial distances plotted horizontally correspond to radii of the spherical shells of integration. The lower graph gives the extent of orbital coverage for each spherical surface of integration.

satellite data are filled with the average spectral power flux calculated from all those volume elements which contain satellite data at the same radial distance. As was noted, incomplete orbital coverage occurred primarily in the sourthern hemisphere. The procedure for artificially filling volume elements with data therefore depends mostly upon the symmetry between the northern and the southern hemispheres. This filling procedure is used because symmetry is found between the northern and the sourthern hemisphere when existing spectral power flux measurements are examined. Finally, volume elements within each radial distance increment are treated as spherical shells with radii which are the average for all measurements within each radial group.

The integration was then performed for 178, 100, and 56.2 kHz, and the result is shown in Figure 3. Each of the radial distances plotted represents an average of the radial distances of the measurements in each corresponding radial distance group. The lower panel in Figure 3 shows the extent of satellite orbital coverage as a percentage of 4π sr. The error bars in the figure represent one standard deviation of the integration for each of 15 spherical shells at each frequency. An interpretation of Figure 3 will be made later in the discussion section of this paper.

Another approach is to examine the data for a $1/R^2$ radial dependence. Except for the plasmapause propagation effects discussed by *Green et al.* [1977], auroral kilometric radiation propagates away from the earth in free space. The radiation should therefore propagate away from the source region with a $1/R^2$ radial dependence. A plot of average power versus earth-centered radial distances along a radial vector that passes through the source region in a given hemisphere can easily be examined for the $1/R^2$ radial dependence. Prior to selecting a radial vector direction for making this plot, the southern and northern hemispheres are examined for symmetry. As was discussed, they are found to be roughly equivalent in structure; therefore the southern hemisphere data can be reflected about the equatorial plane and averaged together with northern hemisphere data to produce a single hemisphere of data with increased orbital coverage.

Because these data are organized in earth-centered coordinates, average spectral power flux can not easily be examined for $1/R^2$ radial dependence until a solid angle is chosen which passes as near as possible to the source region. After the selection of such a solid angle the dependence of spectral power flux on distance may be examined in a single dimension along the corresponding radial vector. The solid angle direction is chosen by examining the MLT and λ_m dependence of the intensity of the radiation. Figure 4 shows intensity-modulated, polar plots of power flux for four radial distance groups. The logarithm of spectral power flux is used to determine the darkness of the plot. The more intense fluxes correspond to the darker regions in each plot. The plots appear to show a cone of emission originating from premidnight magnetic local times and at intermediate magnetic latitudes. The magnetic latitudes of the solid angle which must be determined are selected to range from 30° and 55°. This selection of magnetic latitudes is large enough to include the location of the source region and small enough to avoid the areas of poor orbital coverage at high latitudes.

The selection of a MLT direction is performed by plotting average power versus earth-centered radial distances in various MLT directions. The MLT which best corresponds to that of the source region will show the most intense and most sharply peaked plot because measurements along a radial vector in that MLT will pass closer to the source region than in any other MLT. Plots made in four MLT groups for spectral power fluxes averaged between 30° and 55° λ_m are shown in Figure 5. On the basis of the above discussion the plot between 22 and 24 hours MLT clearly represents the MLT direction of the source region. The peaks for plots in other magnetic local times are less intense and flattened because those points on a flattened peak represent locations which are separated and approximately equidistant from the source region. The solid angle has now been chosen to range from 22 to 24 hours MLT and from 30° to 55° λ_m. This selection best represents the direction of the source region from the center of the earth and avoids the influence of poor orbital coverage at high magnetic latitudes.

The plot of Figure 5 between 22 and 24 hours MLT can now be examined for $1/R^2$ radial dependence. A straight line fit to the trailing edge of the plotted curve for 178 kHz on this log-log graph has a slope of -3.47. Radial distances plotted on the graph are geocentric rather than distances from the source region, thereby increasing the slope of the straight line fit. The distance of the actual source region from the center of the earth can indirectly be found by replotting spectral power flux where the radial distances used are with respect to various possible source locations. An assumed source location which produces the expected slope of -2.0 when spectral power flux is plotted as a function of the distance from this location would then correspond to the actual distance of the source from the center of the earth. An example of the effect of choosing source locations at 2, 3, and 4 R_E for the frequencies examined is shown in Figure 6. The dashed line in each plot represents a $1/R^2$ slope. As possible source locations are cho-

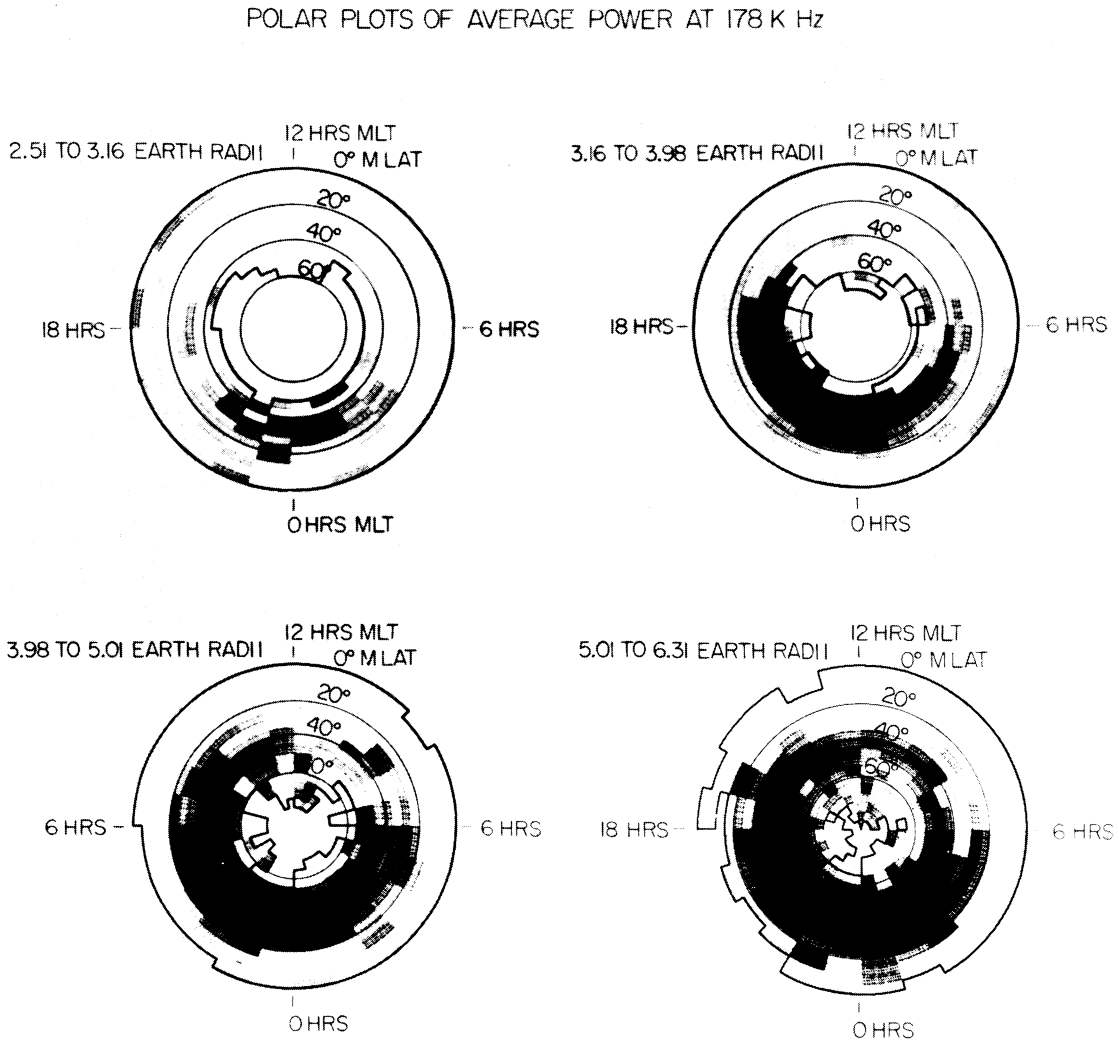

Fig. 4. These are intensity-modulated polar plots of the average spectral power flux observed in four consecutive, concentric, hemispherical shells at 178 kHz. Dark borders interior and exterior to each plot mark the limits of orbital coverage. Plotted intensities are derived from the logarithm of spectral power flux.

sen at consecutively larger distances from the center of the earth, the slope reduces on these log-log plots. A uniform plot of slope as a function of source location is shown in Figure 7. The horizontal dashed line representing a $1/R^2$ slope shows an inferred actual source location which ranges from 2 to 3 R_E.

4. Discussion

The calculation of spectral power emitted at kilometric wavelengths by means of integrating over earth-centered, spherical shells was performed so that the radial distance of the most intense sources of kilometric radiation could be found. The result of the integration in Figure 3 agrees remarkably well with the idealized sketch shown in Figure 2. In many respects, however, the result shown in Figure 3 is not the product of ideal conditions. First, $\mathbf{S} \cdot d\mathbf{A}$ was approximated with the measured spectral power flux PdA or $(\epsilon_0/u_0)^{1/2} E^2 dA$. As a measurement of the spectral poynting flux magnitude $|\mathbf{S}|$, the spectral power flux has been shown to be no more than about a factor of 2 too small. As a result of the approximation, the magnitude of the component of the poynting flux normal to the surface of integration is not known. This means that the total observed spectral power flux magnitude will be used in the integration at each surface element. When the surface of integration has a large radius and completely encloses the source regions, the error associated with the approximation $\mathbf{S} \cdot d\mathbf{A} = |\mathbf{S}|dA$ should be very small, and the result of the integration should be a constant function of radius. As the surfaces of integration no longer completely enclose the source regions, the integral will become roughly proportional to the area of the surface of integration. The important point is that the value of the integral will not be a constant when the radius of the surface of integration becomes less than the distance of the source positions from the center of the earth, independent of any other effects which may be present. The drop-off occurs in Figure 3 at approximately 4 R_E. An additional reduction in the value of the integral occurs due to measurements made inside the propagation cutoff surface, described by *Gurnett* [1974], which is located at about 2 R_E for high latitudes. For the radiation to be propagating in free space the source of intense kilometric radiation must be outside of the propagation cutoff surface, while the integration of spectral power flux places the source region inside of 4 R_E. The primary result of the integrations therefore locate well-confined intense sources of kilometric radiation at a distance of 2–4 R_E from the center of the earth. Effects, in addition to those described above, can cause the value of the integration

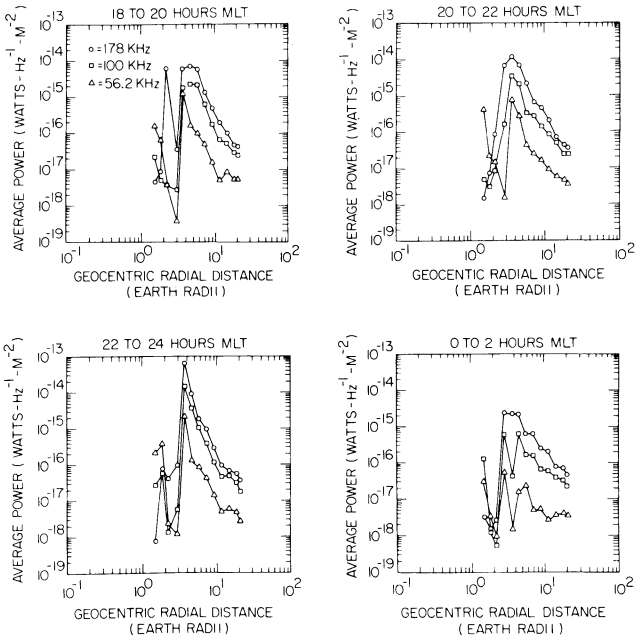

Fig. 5. Average spectral power flux is plotted against geocentric radial distance in four magnetic local time groups. Spectral power has been averaged between 30° and 55° λ_m in each magnetic local time group. The graph from 22 to 24 hours MLT best corresponds to the MLT of the source region of auroral kilometric radiation.

to reduce. The drop-off at 4 R_E is therefore an outer limit to the generation of intense kilometric radiation. No significant source of power at kilometric wavelengths is seen between 5 and 15 R_E.

A measurement of the total power emitted as auroral kilometric radiation can also be determined. The significance of various features of the curves in Figure 3 must be examined before the emitted power can be obtained. Where orbital coverage becomes poor, the error in the integration becomes very large. The error for radial distances less than 3 R_E does not significantly effect the determination of source position because the reduction in the value of the integral remains clearly indicated near 4 R_E. Owing to the large errors at distances beyond 21 R_E, the sharp rise in the value of the integral cannot be reliably interpreted. It is likely that the sharp rise in the integrated power at distances beyond 21 R_E is caused by the sharply reduced orbital coverage (particularly from Hawkeye) and the simultaneous observation of both northern and southern hemispherical sources on the nightside of the earth. At this distance the solid angle where both sources are observable becomes a significant fraction of all solid angles where orbital coverage exists. An observation of spectral power flux is twice as large as that for the observation of only one source. Because the average of spectral power flux from those volume elements where coverage exists (primarily near the equator) is used to fill those volume elements where orbital coverage does not exist (primarily over the poles), the value of the in-

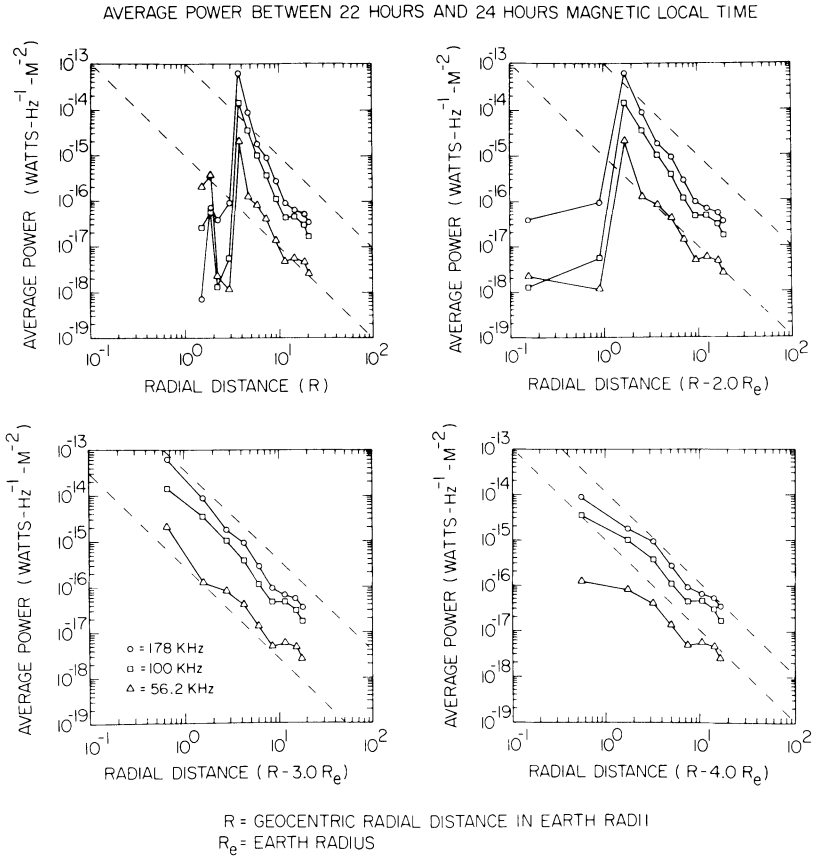

Fig. 6. Average spectral power flux is plotted against the distances from selected possible source locations. All four plots are for spectral power flux which has been averaged between 22 and 24 hours MLT and between 30° and 55° λ_m. Data in the upper left panel are plotted against geocentric radial distances. Points in the other three panels are plotted as a function of the distances away from model source locations at 2, 3, and 4 R_E. The dotted lines which indicate a $1/R^2$ slope show that data plotted for a source location at 3 R_E most nearly follow the $1/R^2$ functional dependence.

tegration of spectral power flux across all solid angles tends to be larger than for the case when both sources could not be simultaneously observed. The slight downward slope of the curves in Figure 3 between 4 and 21 R_E appears to result from the procedure used to compensate for incomplete orbital coverage. As the radius of the spherical surface of integration increases, the satellite coverage in the southern hemisphere changes from positions near the source at intermediate latitudes to positions far from the source at more equatorial latitudes. When data from these southern hemisphere latitudes are averaged into existing northern hemisphere data, the resulting average first overestimates and then underestimates the average of the spectral power flux intensities where there is no orbital coverage. The value of the integration is first above and then below the unbiased value.

The portion of the curves in Figure 3 between 4 and 20 R_E has been averaged to estimate the power produced by both the northern and the southern hemisphere sources of auroral kilometric radiation. The time-averaged spectral powers produced as auroral kilometric radiation are approximately 37 W/Hz at 178 kHz, 16 W/Hz at 100 kHz, and 2 W/Hz at 56.2 kHz. Using a spectrum bandwidth of 200 kHz [see *Kaiser and Alexander*, 1977] for the emission, the total time-averaged power generation by one source is nearly 10^7 W. Although these are order of magnitude estimates, they agree with an estimate of average power generation by *Kaiser and Alexander* [1977] and are compatible with an estimate of the peak power generation of 10^9 W made by *Gurnett* [1974].

The second approach used to determine the auroral kilometric radiation source location is to examine the data for $1/R^2$ radial dependence. As described before, the solid angle is chosen between 30° and 55° λ_m or 57° and 69° invariant latitude and between 22 and 24 hours MLT. These latitudes are compatible with the 65°–70° invariant latitude, which have been found for the auroral source location by *Kurth et al.* [1975]. Once the solid angle is chosen, the results of searching for the effective source location are shown in Figures 6 and 7. Figure 7 shows that radiation from sources located at 2–3 R_E display the expected $1/R^2$ radial dependence at all three of the frequencies studied. The error bars in Figure 7 represent the standard deviation of straight line fits to log-log plots such as those in Figure 6. This error results from the statistical error in the plotted points and the incorporation of electric fields in the data which are not related to auroral kilometric radiation. Although the errors are such that no significance can be drawn from the ordering of the curves in Figure 7, the apparent systematic decrease of source altitude with frequency warrants further study. It should be noted that electric fields unrelated to auroral kilometric radiation are typically more intense at lower frequencies, and this may be the cause of the unexpected ordering of the curves in Figure 7.

In addition to source strength and position, a striking feature of auroral kilometric radiation is the broad angular emission pattern. The intensity modulated plots, like those in Figure 4, have been used to derive a sketch of the emission cone at 178 kHz. Figure 8 shows the cone of emission in the 11- to 23-hour MLT plane overlayed on the Hawkeye magnetic field model of *Chen and Van Allen* [1978]. The plasmasphere shown in the sketch extends to $L = 4$ and is intended to correspond to an average *kp* index of 3+. The borders of the emission pattern are defined by a drop of 2 or more orders of magnitude in the observed spectral power flux for each spherical shell into which the data have been averaged. The emission

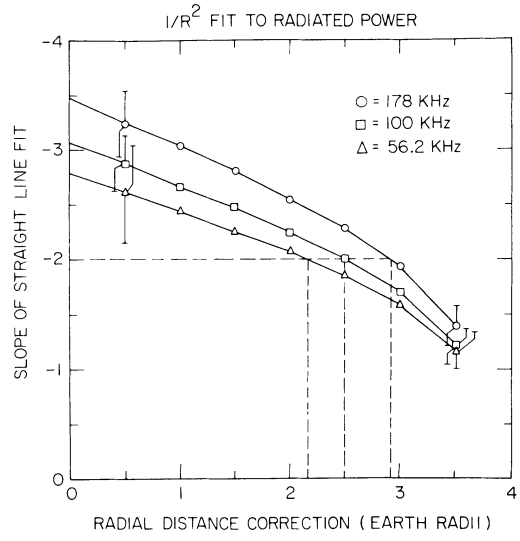

Fig. 7. The slopes of straight line fits to the data are plotted against the geocentric distances of model source positions. Spectral power flux falls off as $1/R^2$ for a model source positioned between 2 and 3 R_E.

pattern is almost 180° wide in the dawn-dusk plane, crosses the equatorial plane near 12 R_E on the nightside of the earth, and is as low as 45° λ_m at 10 R_E on the dayside. Ray tracing in a model plasmasphere of $L = 4$ for a source at 2.3 R_E and 178 kHz was performed by J. L. Green (private communication, 1978) and confirms the sketch in Figure 7. By examining spectral power flux also at 100 and 56.2 kHz the solid angles of the illumination patterns are found to be about 4.1 sr at 178 kHz, 2.2 sr at 100 kHz, and 1.5 sr at 56.2 kHz. These emission cone solid angles confirm those found by *Green et al.* [1977], who developed frequency of occurrence pictures in MLT and λ_m for the observations of auroral kilometric radiation. Using a drop in the frequency of occurrence to 50% to define emission cone boundaries, Green estimated emission cone solid angles to be 3.5 sr at 178 kHz, 1.8 sr at 100 kHz, and 1.1 sr at 56.2 kHz.

Only the auroral sources of kilometric radiation are clearly observed using these methods of analysis. They are well-confined near 65° invariant latitude in their respective hemispheres, from 22 to 24 hours MLT, and between 2 and 3 R_E. On the average, instantaneous sources of auroral kilometric radiation must also be confined within this region, because it is the variation in the location of instantaneous sources which gives the appearance of an extended region of power generation.

No sources of power are evident in Figure 3 between 5 and 15 R_E. As was discussed, the downward slope in the figure results from using the average of observed spectral power flux on a given shell as a substitute for actual spectral power flux values where there are no observations. The largest statistical error in the integration between 5 and 15 R_E for 178 kHz is approximately ±20%. To be observed in this region of Figure 3 a source of electromagnetic radiation at 178 kHz would need to generate an average power equal to or greater than 20% of the power generated as auroral kilometric radiation. Observations of dayside sources at distances greater than 5 R_E by *Kaiser and Stone* [1975] show that the flux from these sources is much less than that from the auroral sources of kilometric radiation. These sources are too weak to be observed by this

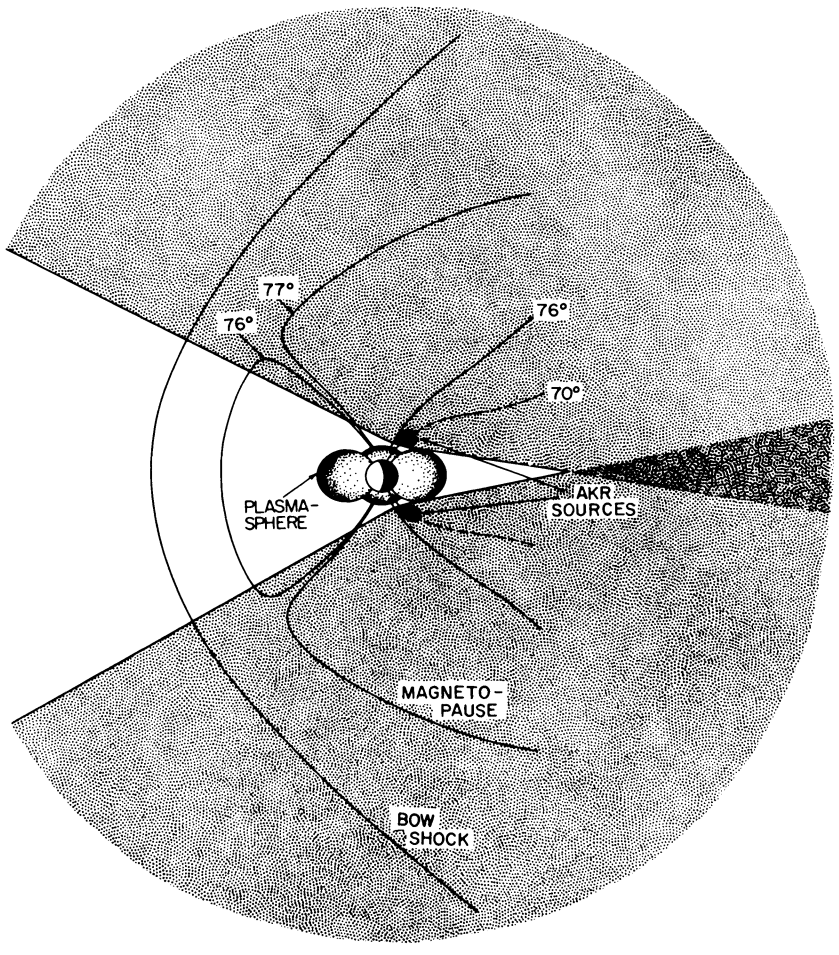

Fig. 8. The time-averaged extent of the conelike emission of auroral kilometric radiation is shown along with the Hawkeye magnetic field model of *Chen and Van Allen* [1978]. On the average, both sources are observable in the equatorial plane on the nightside of the earth at a distance of 12 R_E and beyond. The polar cusp is illuminated by auroral kilometric radiation at radial distances as close as 4 R_E.

study. A more detailed study of the characteristics of the integration of spectral power flux is needed before the nature of kilometric radiation sources between 5 and 15 R_E can be determined. However, the observed illumination of the polar cusp at distances as small as 4 R_E allows observations of polar cusp sources, such as those by *Alexander and Kaiser* [1976], to be explained by scattering from field-aligned density irregularities.

5. Conclusions

Intense sources of power radiating at kilometric wavelengths are found near 65° invariant latitude in the northern and southern hemispheres, from 22 to 24 hours MLT, and between 2 and 4 R_E. These dominant sources of power produce the electromagnetic radiation that has been described by *Kurth et al.* [1975] as auroral kilometric radiation. Each northern and southern hemisphere auroral kilometric radiation source is well confined and emits radiation into solid angles of about 4.1 sr at 178 kHz, 2.2 sr at 100 kHz, and 1.5 sr at 56.2 kHz. A lower limit for the spectral power generated by each source is found to be 37 W/Hz at 178 kHz, 16 W/Hz at 100 kHz, and 2 W/Hz at 56.2 kHz. For a bandwidth of 200 kHz the total time-averaged power emitted by the northern and southern sources of auroral kilometric radiation is found to be about 10^7 W.

Acknowledgments. We wish to extend special thanks to J. L. Green, W. S. Kurth, and R. R. Anderson for their valuable advice. This work was supported by NASA under grant NGL-16-001-043 and contracts NAS5-11074, NAS5-11431, and NAS1-13129.

The Editor thanks J. Alexander and M. S. Frankel for their assistance in evaluating this paper.

References

Alexander, J. K., and M. L. Kaiser, Terrestrial kilometric radiation, 1, Spatial structure studies, *J. Geophys. Res., 81,* 5948, 1976.

Alexander, J. K., M. L. Kaiser, and P. Rodriguez, Scattering of terrestrial kilometric radiation at very high altitudes, *J. Geophys. Res., 84,* 2619, 1979.

Benediktov, E. A., G. G. Getmantsev, Yu. Al. Sazonov, and A. F. Tarasov, Preliminary results of measurement of the intensity of distributed extraterrestrial radio-frequency emission at 725 and 1525-kHz frequencies by the satellite Elektron-2, *Cosmic Res.,* English Transl., *3,* 492, 1965.

Benediktov, E. A., G. G. Getmantsev, N. A. Mityakov, V. O. Papoport, and A. F. Tarasov, Radiation between geomagnetic activity and the sporadic radio emission recorded by the Elektron satellites, *Cosmic Res.,* Engl. Transl., *6,* 791, 1968.

Chen, T.-F. and J. A. Van Allen, The earth's magnetic field at large radial distances as observed by Hawkeye 1, submitted to *J. Geophys. Res.,* 1978.

Dunckel, N., B. Ficklin, L. Rorden, and R. A. Helliwell, Low-frequency noise observed in the distant magnetosphere with Ogo 1, *J. Geophys. Res., 75,* 1854, 1970.

Green, J. L., D. A. Gurnett, and S. D. Shawhan, The angular distri-

bution of auroral kilometric radiation, *J. Geophys. Res., 82,* 1825, 1977.

Gurnett, D. A., The earth as a radio source: Terrestrial kilometric radiation, *J. Geophys. Res., 79,* 4227, 1974.

Gurnett, D. A., and J. L. Green, On the polarization and origin of auroral kilometric radiation, *J. Geophys. Res., 83,* 689, 1978.

Gurnett, D. A., and R. R. Shaw, Electromagnetic radiation trapped in the magnetosphere above the plasma frequency, *J. Geophys. Res., 78,* 8136, 1973.

Kaiser, M. L., and J. K. Alexander, Terrestrial kilometric radiation, 3, average spatial properties, *J. Geophys. Res., 82,* 3273, 1977.

Kaiser, M. L., and R. G. Stone, Earth as an intense planetary radio source: Similarities to Jupiter and Saturn, *Science, 189,* 285, 1975.

Kaiser, M. L., J. K. Alexander, A. C. Riddle, J. B. Pearce, and J. W. Warwick, Direct measurements by Voyagers 1 and 2 of the polarization of terrestrial kilometric radiation, *Geophys. Res. Lett., 5,* 857, 1978.

Kurth, W. S., M. M. Baumback, and D. A. Gurnett, Direction-finding measurements of auroral kilometric radiation, *J. Geophys. Res., 80,* 2764, 1975.

Stone, R. G., Radio physics of the outer solar system, *Space Sci. Rev., 14,* 534, 1973.

(Received February 12, 1979;
revised May 17, 1979;
accepted June 21, 1979.)